CHIN.PHYS.LETT. Vol. 20, No. 11 (2003) 2019

First-Principles Calculations of Scanning-Tunnelling-Microscopy Images of Ar Atoms Adsorbed on a Graphite Sheet *

BAI Yu-Lin(白玉林)[1,2], ZHOU Xiao-Lin(周晓林)[1,3], CHEN Xiang-Rong(陈向荣)[1**], GOU Qing-Quan(苟清泉)[1]

[1]*Institute of Atomic and Molecular Physics, Sichuan University, Chengdu 610065*
[2]*Department of Science and Technology of Electronic Information, Yibin University, Yibin 644000*
[3]*Department of Physics, Sichuan Normal University, Chengdu 610066*

(Received 9 June 2003)

Local density approximation within the framework of the density functional theory is applied to calculate the scanning tunnelling microscopy (STM) images of Ar atoms adsorbed on a graphite sheet (Ar/graphite system). It is found that the optimal site of adsorbed Ar atom is at the top of the centre of the carbon hexagon and its equilibrium distance from the graphite surface is about 3.20 Å. We demonstrate that it is the hybridization of the C 2p electronic states with the Ar 3p and 4s electronic states, which renders Ar atoms visible in the STM experiment.

PACS: 73.20.At, 31.15.Ew, 81.05.Tp, 87.64.Dz

Scanning tunnelling microscopes (STMs)[1,2] have become a powerful tool in surface science to imaging of various adsorbate atoms and molecules on atomically flat surfaces since the invention. In the constant-tunnelling current mode,[2] the STM image is given by recording the tip-to-surface distance changes. In the current-imaging mode,[3] however, an STM image is given by recording the tunnelling current as the tip rapidly scans the surface at a constant distance. In most cases, STM images can be associated with the topography of the electronic states of materials, such as Si (111)-7 × 7.[4] In some cases, STM images show the electronic structure efforts and form different patterns instead of real topography, e.g., graphite is the most well known material.[5]

Over the past few years, adsorbate-induced substrate modifications have attracted great interest in the field of surface science,[6−9] and the rare-gas atom, as an adsorbate, has a long tradition in serving as a model system due to its simple electronic structure and the weak interaction with the substrate. According to the theory of Tersoff and Hamann,[10] whether or not adsorbate atoms and molecules are visible in the STM experiment depends on how it modifies the LDOS near the Fermi level. The rare-gas atoms adsorbed on the metal and graphite surface, however, are unlikely to modify the LDOS near the Fermi level since the energies of the highest filled states of the rare-gas atom are much lower and those of the lowest-lying empty states are much higher than the Fermi level. Hence, it was surprising to find that rare-gas atoms are visible in the STM experiments.[11−13]

Eigler *et al.*[11] have used the atom-on-jellium model to account for the STM images of rare-gas Xe atoms absorbed on Ni(110) (Xe/Ni(100) system). Mingo *et al.*[14] have introduced a theory based on the Keldysh Green function formalism for the STM current of the Xe/Ni(100) and Xe/Al(100) systems. They all have argued that the resonance of the empty Xe 6*s* state is the principal origin of the Fermi-level LDOS. Recently, we have applied first-principles calculations to the STM images of Kr and Xe atoms adsorbed on a monolayer graphite surface.[15,16]

It is of interest to compare the behaviour of rare gases argon, krypton and xezon when physisorbed on graphite surfaces. We know that, the atom–atom and atom-substrate interactions are similar in the three cases.[17] Here we focus on the Ar/graphite system. We apply the first-principles calculations to the study of the STM images for a commensurate $(\sqrt{3}\times\sqrt{3})R30^\circ$ Ar phase of the Ar/graphite system.

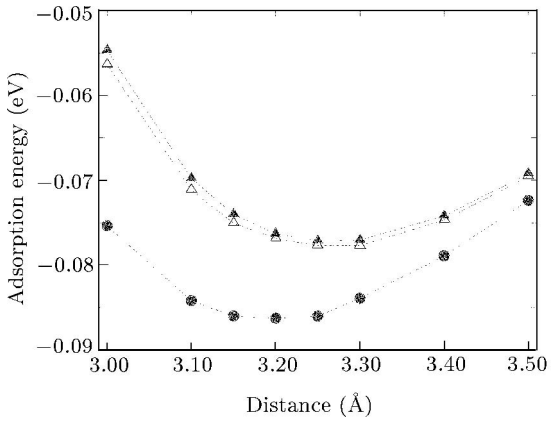


Fig. 1. Distances between Ar atom and graphite surface versus the adsorption energy of the Ar/graphite system. Closed circle, closed triangle and open triangle denote the C (top of the centre of the carbon hexagon), B (top of the centre of the C-C bond), and T (top of a carbon atom) sites, respectively.

* Supported by the National Natural Science Foundation of China under Grant No 10274055, and the Scientific Research Foundation for the Returned Overseas Chinese Scholars of the Ministry of Education of China.

** To whom correspondence should be addressed.

©2003 Chinese Physical Society and IOP Publishing Ltd

All the studies have been performed using the local density approximation (LDA) within the framework of the density functional theory (DFT).[18,19] The atom-adsorbed graphite sheet is simulated by a repeating slab model, in which the graphite layers are separated substantially to avoid artificial interactions. For the exchange-correlation energy among electrons, we use a functional form[20] fitted to the Monte Carlo results for the homogeneous electron gas.[21] Norm-conserving pseudopotentials generated by using the Troullier–Martins scheme are adopted to describe the electron–ion interaction.[22,23] In constructing the pseudopotentials, core radii adopted are 1.50 a.u., 1.54 a.u., and 1.54 a.u. for the C $2s$, $2p$, and $3d$ states, respectively, and 1.65 a.u., 1.65 a.u., and 1.65 a.u. for the Ar $3s$, $3p$ and $3d$ states, respectively. The valence wavefunctions are expanded by the plane-wave basis set with a cut-off energy of 50 Ry, which gives enough convergence of relative total energies of carbon-related system.[22] The conjugate-gradient minimization scheme is used both for the self-consistent electronic structure calculations and for the geometry optimization. Integrations over the surface Brillouin zone are carried out using an 8-k-point sampling with one-k-point in the z direction in the self-consistent calculations. Detailed accounts for the computational method have been seen elsewhere.[24,25]

First, the present method is applied to a graphite surface. The equilibrium lattice constant obtained is 4.213 Å with accuracy of 1.1% compared with the experimental value, 4.260 Å. The optimal site for the adsorbed Ar atom and its equilibrium distance from the graphite surface are then determined by the full geometrical optimizations for the commensurate $(\sqrt{3}\times\sqrt{3})R30^\circ$ structure of the Ar/graphite system. Here, three different possible adsorption sites, i.e. the C (top of the centre of the carbon hexagon), B (top of the centre of the C–C bond), and T (top of a carbon atom) sites, have been considered. In all the calculations, we ignore the effect of metal tip on Ar atoms in the STM experiment. The results obtained are shown in Fig. 1.

We find that the C site with the equilibrium distance of about 3.20 Å from the graphite surface is the most stable for the Ar adsorption. The corresponding equilibrium distances from the graphite surface for the B and T sites are 3.30 Å and 3.25 Å, respectively. The differences in total energy are both about 9 meV between the C and B sites and between the C and T sites, indicating that the commensurate-incommensurate (CI) structural transition is easy to occur for Ar atoms adsorbed on graphite surface even at low temperature. In this study, we only consider the C site with the equilibrium distance, 3.20 Å, and the corresponding adsorption energy, 86 meV. The results obtained agree well with those obtained by Zhao *et al.*[26] and with the best estimated experimental data.[27] For Kr/graphite and Xe/graphite systems, the equilibrium distances are 3.35 Å and 3.60 Å with the corresponding adsorption energy 160 meV and 204 meV, respectively. It is indicated that the attractive interaction between Xe atom and graphite surface is the largest among them. Our studies show that the Xe/graphite system is like a chemisorbed system, just similar to the Xe/Ni(100) and Xe/Al(100) systems,[14] as is not of our focus here.

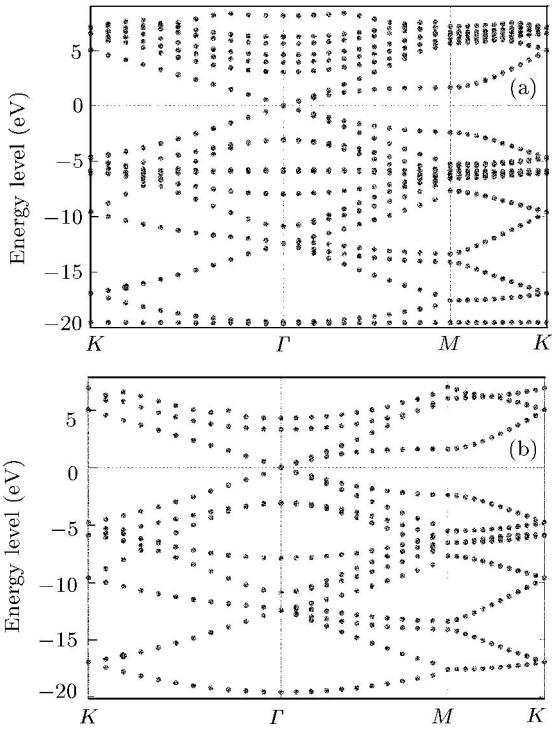


Fig. 2. Calculated electronic band structures for: (a) Ar/graphite system, (b) graphite surface. Energy levels are relative to the Fermi level.

The calculated electronic band structures for the Ar/graphite system and for the $(\sqrt{3}\times\sqrt{3})R30^\circ$ structure of graphite surface are shown in Fig. 2. We note that the top of the valence bands and the bottom of the conduction bands for the Ar/graphite system and the $(\sqrt{3}\times\sqrt{3})R30^\circ$ graphite surface are both at Γ point and the four energy bands of π-electrons are degenerate at Γ point, as is different from that of 1×1 graphite surface.[28] For the 1×1 graphite surface, the degeneracy appears at K point, which is folded at Γ point in the $(\sqrt{3}\times\sqrt{3})R30^\circ$ periodicity.

To calculate the STM images of the Ar/graphite system, we use the following expression for tunnelling current density[25]

$$j_{\pm}(\boldsymbol{r},V)=\pm\int_{E_F\mp|V|}^{E_F}\sum_{nk}|\psi_{nk}(\boldsymbol{r})|^2\delta(E-E_{nk})\mathrm{d}E, \tag{1}$$

where $\psi_{nk}(r)$ and E_{nk} represent the wavefunction and the corresponding eigenvalue for the state with the band index n and the wavenumber k; while $\boldsymbol{r}$ is the position of the STM tip, and V is the applied bias voltage between the tip and the sample. The $\pm$ signs

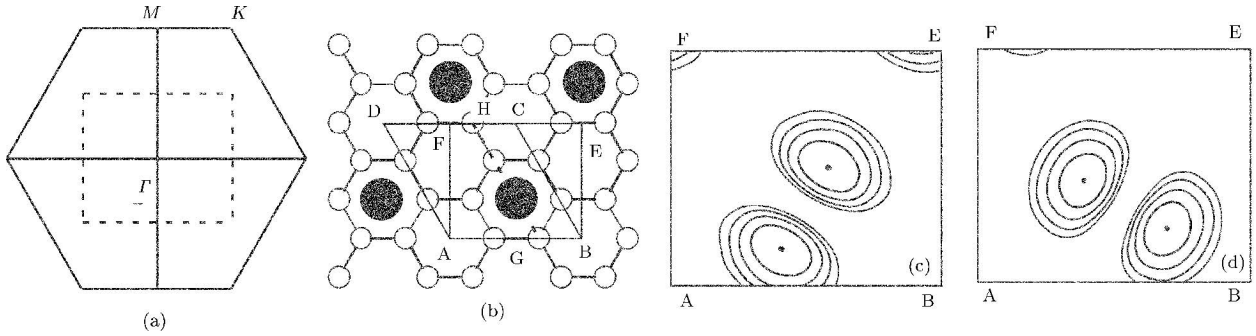


Fig. 3. (a) Hexagonal Brillouin zone of the Ar/graphite system. The 99 k-points adopted for the STM calculations are in the rectangular area near point. (b) The schematic diagram of the Ar/graphite system, where the rhombus ABCD denotes the unit cell. The rectangle ABEF corresponds to the plane on which the STM images are shown. The solid and open circles denote the sites of Ar and C atoms, respectively. The calculated STM images (tunnelling current density) for the Ar/graphite system at the sample bias voltages of (c) $V = -1\,\mathrm{eV}$, (d) $V = 1\,\mathrm{eV}$ (for the case of only Γ point used). The subsequent contours differ by a factor of 1.5.

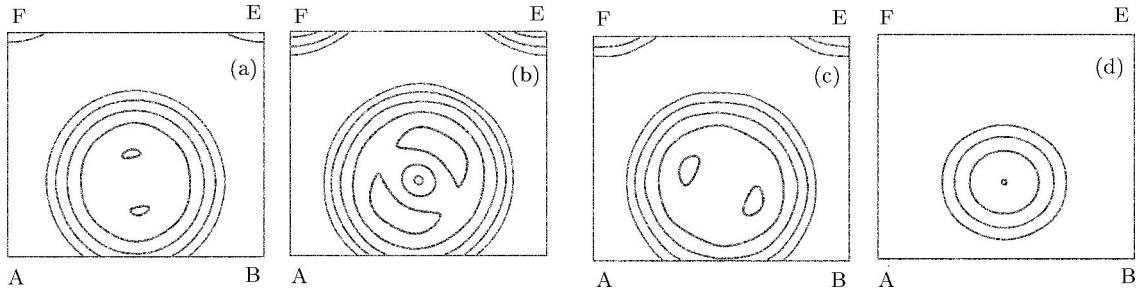


Fig. 4. Calculated STM images (tunnelling current density) for the Ar/graphite system at the sample bias voltages of (a) $V = -2\,\mathrm{eV}$, (b) $V = -1\,\mathrm{eV}$, (c) $V = 1\,\mathrm{eV}$, and (d) $V = 2\,\mathrm{eV}$ (for the case of 99 k-points used). The subsequent contours differ by a factor of 1.5.

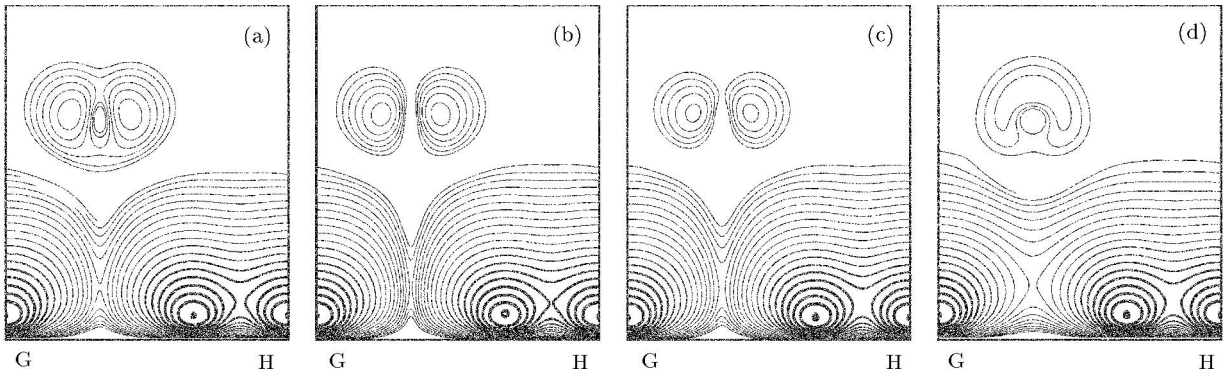


Fig. 5. Contour plots of local density of state for the Ar/graphite system on a plane perpendicular to the graphite surface at the sample bias voltages of (a) $V = -2\,\mathrm{eV}$, (b) $V = -1\,\mathrm{eV}$, (c) $V = 1\,\mathrm{eV}$, and (d) $V = 2\,\mathrm{eV}$. The plane with the height of 12 Å includes the dashed line GH in Fig. 3(b). The subsequent contours differ by a factor of 1.5.

denote the filled-state and empty-state STM images corresponding to the negative and positive sample bias voltage, respectively.

The calculations for the STM images are performed in the following two cases: (i) using only Γ point, (ii) using 99 k-points that are sampling the $\boldsymbol{k}$-space region near the Fermi level in the rectangular area in surface Brillouin zone [see Fig. 3(a)]. From Fig. 2, we know that the Fermi surface of this system lies close to the Γ point in the surface Brillouin zone. In the first case, only one k-point (i.e. the Γ point) contributes to the STM images at the Fermi level. In the second case, however, a very fine mesh of 99 k-points near Γ point are used, since they make the main contributions to the STM images near the Fermi level.

All the obtained results are shown in Figs. 3(c)–3(d) and Figs. 4(a)–4(d), respectively. They are obtained on the typical plane parallel to the graphite surface with the distance of 4.5 Å (the height is about 1.3 Å above the adsorbed Ar atom. The increase of the height does not affect the results, but affect the brightness of the STM images, as is seen obviously from Fig. 5. Comparing to that of the STM

experiment of graphite,[29] we think that the chosen height seems to be enough for our studies). Figure 3(b) shows the schematic diagram (parallel to the graphite surface) of the Ar/graphite system, where the rhombus ABCD denotes the unit cell; the rectangle ABEF corresponds to the plane on which the STM images are shown; the solid and open circles denote the sites of Ar and C atoms, respectively. For these calculations, we take the spacing of two adjacent graphite sheets in the slab model to be 18.0 Å to avoid the interactions between graphite surfaces.

For the filled-state image of the first case, we find that the peak position in the tunnelling current density is located on the top of Ar atom forming a p-like orbital pattern. When the sample bias voltage is changed with other small negative values, we are unable to find any change in the filled-state images. On the other hand, for the empty-state image, the peak position is also located on the top of Ar atom, but a p-like orbital pattern forms in a different direction. The changes of the sample bias voltage also do not affect empty-state images. These results clearly indicate that Ar $3p$ state contributes to the LDOS near the Fermi level of the Ar/graphite system. Lang[30] has studied a single atom which adsorbates on metal surfaces. He has shown that the crucial parameters in determining the low-bias STM images are the s-state or p-state densities due to the adsorbate at the Fermi level, with which our results are consistent.

In the second case, similarly to the discussions above, the peak positions are also located on the top of the Ar atom for both filled- and empty-state images, but the peak positions form elongated circles in different directions. Obviously, this is due to the Ar $3p$ states. As the positive bias voltage is increased from 1 eV to 2 eV, the elongated circles become nearly regular circles, which indicates that, besides Ar $3p$ states, Ar $4s$ state also contribute to the LDOS near the Fermi level of the Ar/graphite system.

In both the positive and negative bias voltages, carbon atoms are invisible because of the large distance between the STM tip and the graphite surface. To clarify the results obtained, we show the contour plots of the LDOS on the plane normal to the graphite surface in Fig. 5. We note that the filled states near the Fermi level are mixed with p orbitals at the Ar site, whereas the empty states are mixed with more s-like orbitals. This finding is in good agreement with the notion that the filled states are mixed with Ar $3p$ state, whereas the Ar $3p$ and $4s$ states contribute to the empty states near the Fermi level.

These results suggest that the attractive interaction between the Ar atom and the graphite surface, resulting from the hybridization of the C $2p$ electronic states (π-electronic states) and the Ar $3p$ and $4s$ electronic states, will strongly broaden the adsorbed Ar $3p$ and $4s$ energy levels, which is therefore overlapping with the Fermi level. Although the overlap is small, its effect is to increase substantially the hybridization contribution to the LDOS of Ar/graphite system near the Fermi level. Hence, we conclude that the STM images of the Ar/graphite system are mainly due to the hybridization of the C $2p$ electronic states (π-electronic states) with the Ar $3p$ and $4s$ electronic states.

All the calculations are performed on a Fujitsu VPP5000 computer of Science Information Processing Center in University of Tsukuba.

References

[1] Binnig G, Rohrer H, Gerber Ch and Weibel E 1982 *Appl. Phys. Lett.* **40** 178
[2] Binnig G, Rohrer H, Gerber Ch and Weibel E 1982 *Phys. Rev. Lett.* **49** 57
[3] Bryant A, Smith D P E and Quate C F 1986 *Appl. Phys. Lett.* **48** 832
[4] Binnig G, Rohrer H, Gerber Ch and Weibel E 1983 *Phys. Rev. Lett.* **50** 120
[5] Hockett L A and Creager S E 1993 *Rev. Sci. Instrum.* **64** 263
[6] Somorjai G 1994 *Introduction to Surface Chemistry and Catalysis* (New York: Wiley)
[7] He P M et al 2001 *Chin. Phys. Lett.* **18** 97
[8] Jin P, Meng X Q, Zhang Z Y and Li C M 2002 *Chin. Phys. Lett.* **19** 1010
[9] Wang P et al 2002 *Chin. Phys. Lett.* **19** 409
[10] Tersoff J and Hamann D R 1983 *Phys. Rev. Lett.* **50** 1998
Tersoff J and Hamann D R 1985 *Phys. Rev.* B **31** 805
[11] Eigler D M, Weiss P S, Schweizer E K and Lang N D 1991 *Phys. Rev. Lett.* **66** 1189
[12] Grimm B, Hövel H, Pollmann M and Reihl B 1999 *Phys. Rev. Lett.* **83** 991
[13] Matsui T, Kambara H and Fukuyama H 2002 *J. Low Temp. Phys.* **126** 373
[14] Mingo N, Jurczyszyn L, Garcia-Vidal F J and Saiz-Pardo R 1996 *Phys. Rev.* B **54** 2225
[15] Chen X R, Oshiyama A and Okada S 2003 *Phys. Rev.* B **67** 033408
[16] Chen X R *et al* 2003 *Phys. Lett.* A **315** 403
[17] Steele W A 1973 *Surf. Sci.* **36** 317
Price G L 1974 *Surf. Sci.* **46** 697
[18] Hohenberg P and Kohn W 1964 *Phys. Rev.* B **136** 864
[19] Kohn W and Sham L J 1965 *Phys. Rev.* **140** A1133
[20] Perdew J P and Zunger A 1981 *Phys. Rev.* **B23** 5048
[21] Ceperley D M and Alder B J 1980 *Phys. Rev. Lett.* **45** 566
[22] Troullier N and Martins J L 1991 *Phys. Rev.* B **43** 1993
[23] Kleinman L and Bylander D M 1982 *Phys. Rev. Lett.* **48** 1425
[24] Okada S, Saito S and Oshiyama A 2002 *Phys. Rev.* B **65** 165410 and references therein
[25] Yu B D, Ide T and Oshiyama A 1994 *Phys. Rev.* B **50** 14631
[26] Zhao J, Buldum A, Han J and Lu J P 2002 *Nanotechnol.* **13** 195
[27] Vidali G, Ihm G, Kim H Y and Cole M W 1991 *Surf. Sci. Rep.* **12** 133 and references therein
[28] Chen X R, Oshiyama A, Okada S and Gou Q Q 2003 *Chin. Phys. Lett.* **20** 404
[29] Tománek D and Louie S G 1988 *Phys. Rev.* B **37** 8327
[30] Lang N D 1986 *Phys. Rev. Lett.* **56** 1164
Lang N D 1987 *Phys. Rev. Lett.* **58** 45